631 ESTIMATION OF REGIONAL CLIMATE CHANGES IN EUROPEAN AND MEDITERRANEAN SUBREGIONS USING DIFFERENT RCP SCENARIOS

Rita Pongrácz*, Judit Bartholy, Ildikó Pieczka, Karolina Szabóné André
Dept. of Meteorology, Eötvös Loránd University, Budapest, Hungary

1. INTRODUCTION

In the framework of the Med-CORDEX international initiative of the CORDEX (Coordinated Regional Climate Downscaling Experiment) program within the WCRP (World Climate Research Program), our research group is contributing with RegCM4.3 experiments at 50 km horizontal resolution using the mosaic-type subgridding option in order to take into account subgrid processes. For this purpose, we used ERA-Interim data (1981-2010) and HadGEM2 global model outputs (1951-2005, 2006-2100) as initial and lateral boundary conditions (ICBC) for the entire MED-44 CORDEX area (Fig. 1, upper panel) covering the extended Mediterranean region of Europe (30°-50°N, 10°W-45°E). On the basis of 50 km RegCM runs we aim to provide detailed regional scale climate projection results for the Carpathian Region and its vicinity. For this purpose, further downscaling is necessary using 10 km as horizontal resolution for a smaller domain covering Central Europe with special focus on the Carpathian Region (Fig. 1, lower panel). These experiments will be the basis of the Hungarian national climate and adaptation strategies for detailed regional scale analysis and specific impact studies.

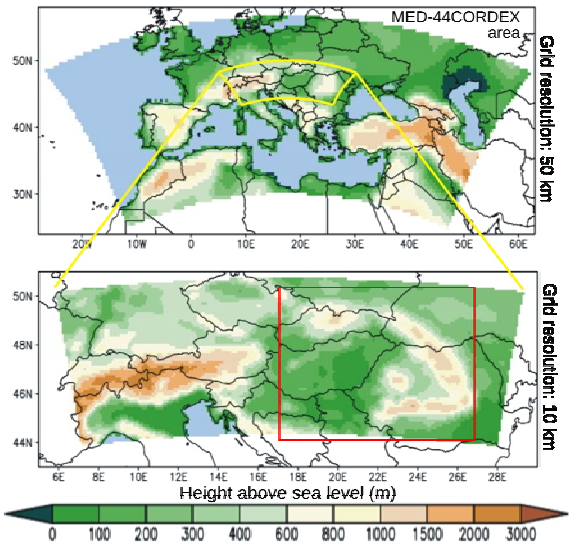

Fig. 1: Topography of the integration domains for the RegCM4.3 simulation at 50 km (top) and 10 km (bottom) horizontal resolution. The red rectangle indicates the Carpathian Region, the main focus area of the 10 km resolution experiment.

The domain of our earlier fine resolution RegCM experiments (Bartholy et al., 2009; Pongrácz et al., 2010; Torma et al., 2011) has been substantially extended from 12000 gridcells to about 25000 gridcells, moreover, in the previous study we used RegCM3 model version, and emission scenarios (Nakicenovic and Swart, 2000) instead of the new Representative Concentration Pathways (RCP) scenarios (van Vuuren et al., 2011).

The model validation results are discussed in Bartholy et al. (2015) using two different ICBCs, (i) from datasets of ERA-Interim reanalysis, and (ii) from simulation outputs of HadGEM2 global climate model (GCM). After completing these historical experiments, future scenarios for the 21st century are run taking into account RCP4.5 and RCP8.5 scenarios, which are based on the radiative forcing change by 2100. In this paper, the projection results are compared for the estimated temperature and precipitation changes for the following 10 subregions of the MED-44 CORDEX area: Alps, Appennin Peninsula, Balkan Region, Middle European Plain, Iberian Peninsula, Carpathian Mountains, Carpathian Basin, East European Plain, Asia Minor, Western Europe. Besides the mean annual, seasonal and monthly projected changes, the potential shifts of the distributions are also analyzed. Besides the mean annual, seasonal and monthly projected changes, the potential shifts of the distributions are also analyzed.

2. REGIONAL CLIMATE MODEL REGCM

Regional climate model RegCM originally stems from the National Center for Atmospheric Research/ Pennsylvania State University (NCAR/PSU) Mesoscale Model version MM4 (Dickinson et al., 1989; Giorgi, 1989). It is a 3-dimensional, limited-area, hydrostatic, compressible, sigma-p vertical coordinate model maintained at ICTP (International Centre for Theoretical Physics), Trieste. It was originally developed by Giorgi et al. (1993a, 1993b) and later modified and improved by Giorgi and Mearns (1999) and Pal et al. (2000). Description of model equations and possible parameterizations available in the latest version can be found in Elguindi et al. (2011) in detail. In our simulations we used the model settings agreed as default within the Med-CORDEX project (Somot et al., 2012) at 50 km horizontal resolution, with the modification of activating the subgrid Biosphere-Atmosphere Transfer Scheme (BATS). Therefore, the land surface processes are modelled by BATS version

* *Corresponding author address*: Rita Pongrácz, Dept. of Meteorology, Eötvös Loránd University, Pázmány st. 1/a. Budapest, H-1117; Hungary; e-mail: prita@nimbus.elte.hu

1e (Dickinson et al., 1993) with the treatment for subgrid variability of topography, and land cover is determined using a mosaic-type approach (Giorgi et al., 2003). Each grid cell is divided into 25 subgrid cells. As a result, in our simulation the size of the land surface grid cell is 10 km × 10 km horizontally.

For the detailed regional analysis several subregions are defined within the integration domain (Fig. 2).

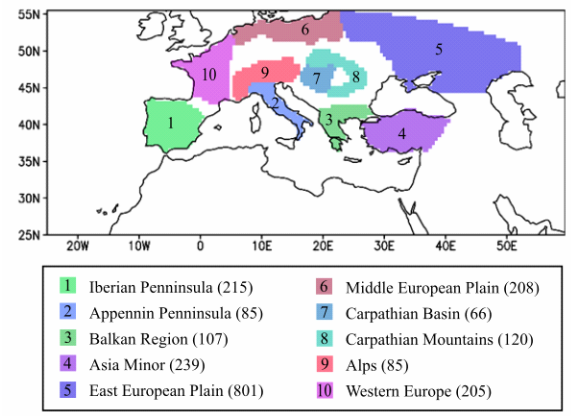

Fig. 2: Subregions within the integration domain defined for regional scale analysis for the 50-km model runs. The numbers appearing in parentheses after the name of the subregion indicate the total number of gridcells within the subregion.

3. PROJECTION RESULTS

After completing the validation analysis (Bartholy et al., 2015) of the two different historical experiments using ERA-Interim reanalysis data and HadGEM2 GCM outputs as ICBC, the GCM simulation driven experiment continued with two different scenario conditions starting from 2006 throughout the entire 21st century. In order to analyze the simulation results, the projected temperature and precipitation changes are mapped and compared on annual and seasonal scales for the coming 2-decade-long periods (i.e., 2021-2040, 2041-2060, 2061-2080, and 2081-2100) for both the RCP4.5 and RCP8.5 scenarios. In this paper the projected annual mean changes of temperature and precipitation are shown in Figs. 3 and 4, respectively. The reference period is defined as the last two decades of the 20th century (1981-2000). In case of temperature the warming signal is clearly seen on the maps of Fig. 3. The larger increase of radiative forcing is projected to result in larger warming. Furthermore, the estimated mean warming is generally larger over land than over the sea. The projected annual mean temperature increases of all the target periods are larger than the inter-annual temperature variability in the reference period. Unlike in case of temperature, the projected mean annual precipitation changes are generally smaller than the inter-annual precipitation variability, especially when taking into account the RCP4.5 scenario.

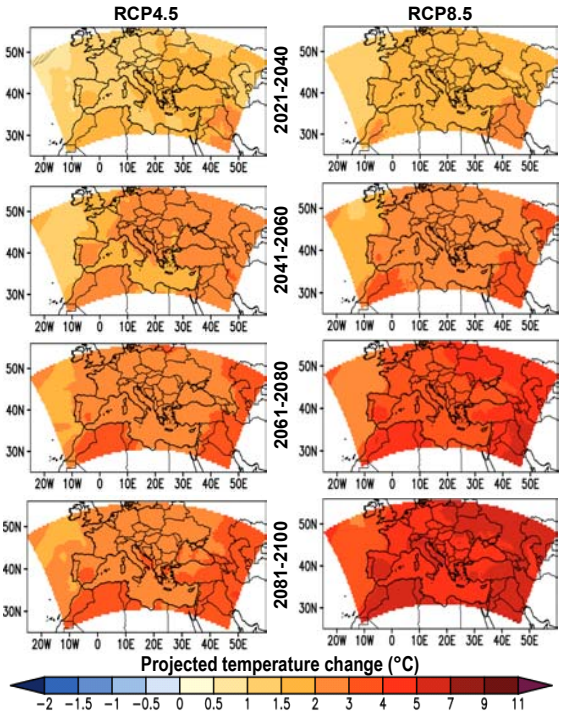

Fig. 3: Projected annual mean temperature changes using the RCP4.5 and RCP8.5 scenarios. The projected warming is larger than the inter-annual variability in the reference period (1981-2000).

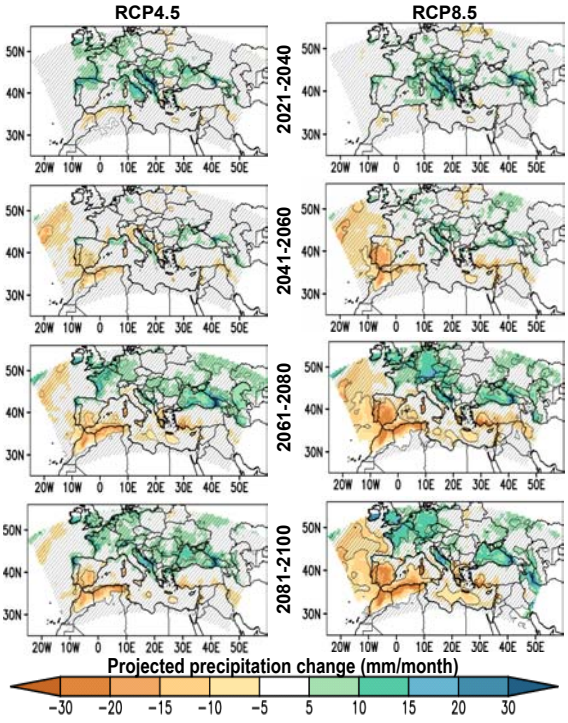

Fig. 4: Projected annual mean precipitation changes using the RCP4.5 and RCP8.5 scenarios. Hatched area indicates where the projected change is smaller than the inter-annual variability in the reference period (1981-2000).

In general, starting from about the mid-century the annual mean precipitation is projected to increase in the northern parts of the domain and decrease in the southern regions.

In addition to the projected mean annual changes, we also calculated the mean seasonal changes for all the four seasons. In case of temperature clear warming trend is projected for all the seasons with slight differences in the spatial pattern. In case of precipitation, seasonal-scale projections are more different for the different seasons than in case of temperature. Precipitation tends to mainly increase in winter and spring, and decrease in summer.

For detailed regional scale analysis Box-Whisker diagrams are used to illustrate the distribution of seasonal mean temperature and precipitation in four different 20-year-long time slices for the future (i.e., 2021-2040, 2041-2060, 2061-2080, and 2081-2100), and thus compared to the reference period of 1981-2000. The diagrams indicate the whole range of the interannual variability (whiskers), and the simulated values around the mean represented by the upper and the lower quartiles (thicker boxes).

For the seasonal mean temperature, results for winter and summer are shown in Figs. 5 and 6, respectively. The projected warming trends are clearly seen in all the subregions. Moreover, although in all seasons (including spring and fall, not shown here) larger warmings are projected when using the RCP8.5 scenario than the RCP4.5 scenario, the difference between the two scenarios are the largest in summer.

For the seasonal mean precipitation, results for all the four seasons are shown in Fig. 7 (winter: December-January-February), Fig. 8 (spring: March-April-May), Fig. 9 (summer: June-July-August), and Fig. 10 (fall: September-October-November), thus the diverse annual differences can be compared. The large spatial variability of precipitation is clearly recognizable in the diagrams. South-North and East-West differences are both present in the estimated precipitation amounts as well, as the projected seasonal changes.

These projection results are certainly affected by the seasonal bias patterns of the historical experiments (Bartholy et al., 2015). In general, the temperature was underestimated in most parts of the entire domain, except at the northeastern part of the domain (e.g., East European Plain) where remarkable overestimation was present for the continental climate. Precipitation was generally overestimated during the historical runs in the entire domain (except in summer). However, RegCM simulation outputs suggest drier climatic conditions in Africa and the Middle East. Moreover, a large underestimation can be found in the eastern part of the domain, especially, in the East European Plain.

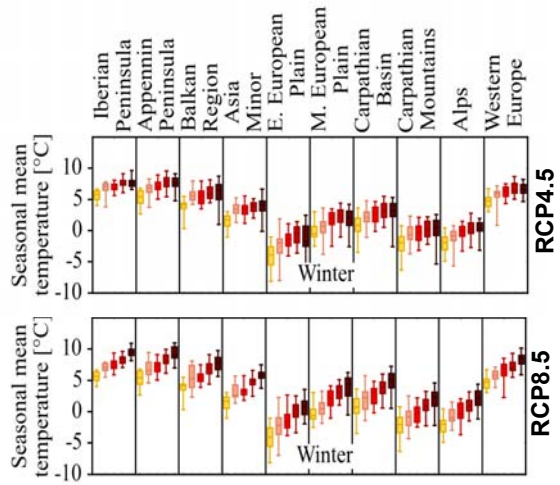

Fig. 5: Box-Whisker diagrams of spatial average values of winter (DJF) mean temperature in the 10 subregions of the MED-44 CORDEX domain calculated from the RCP4.5 (top) and RCP8.5 (bottom) scenario experiments. The presented time slices (indicated from yellow to dark red) are 1981-2000, 2021-2040, 2041-2060, 2061-2080, 2081-2100. The diagrams indicate the whole range of interannual variability (thinner lines), and the simulated values around the mean represented by the upper and lower quartiles (thicker boxes).

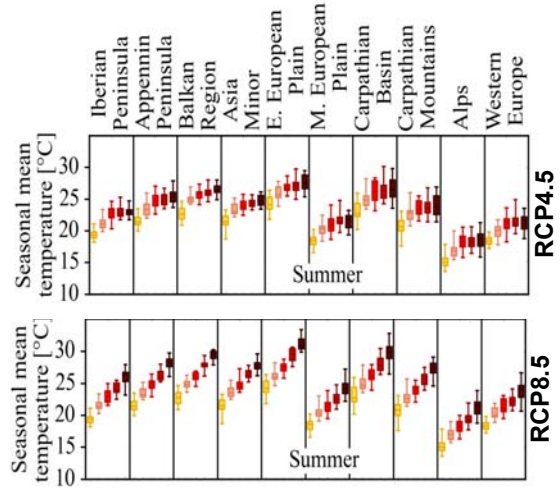

Fig. 6: Box-Whisker diagrams of spatial average values of summer (JJA) mean temperature in the 10 sub-regions of the MED-44 CORDEX domain calculated from the RCP4.5 (top) and RCP8.5 (bottom) scenario experiments. The presented time slices (indicated from yellow to dark red) are 1981-2000, 2021-2040, 2041-2060, 2061-2080, 2081-2100. The diagrams indicate the whole range of interannual variability (thinner lines), and the simulated values around the mean represented by the upper and lower quartiles (thicker boxes).

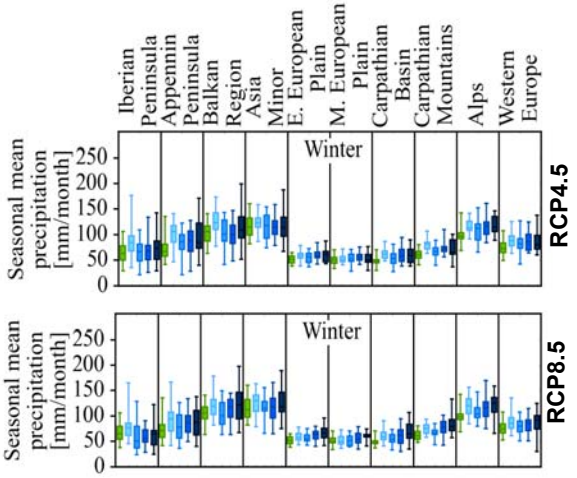

Fig. 7: Box-Whisker diagrams of spatial average values of winter (DJF) mean precipitation in the 10 subregions of the MED-44 CORDEX domain calculated from the RCP4.5 (top) and RCP8.5 (bottom) scenario experiments. The presented time slices (indicated from green to dark blue) are 1981-2000, 2021-2040, 2041-2060, 2061-2080, 2081-2100. The diagrams indicate the whole range of interannual variability (thinner lines), and the simulated values around the mean represented by the upper and lower quartiles (thicker boxes).

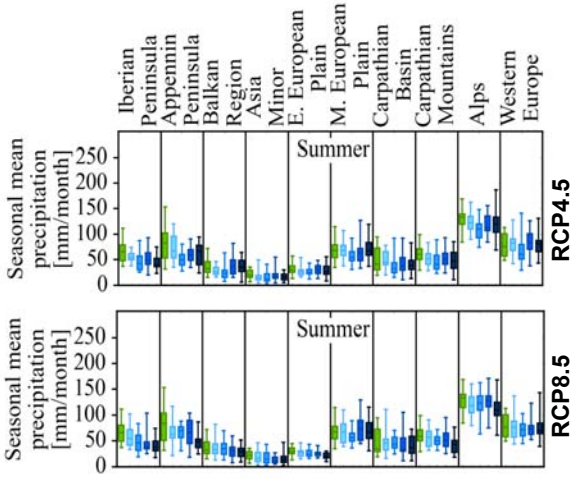

Fig. 9: Box-Whisker diagrams of spatial average values of summer (JJA) mean precipitation in the 10 sub-regions of the MED-44 CORDEX domain calculated from the RCP4.5 (top) and RCP8.5 (bottom) scenario experiments. The presented time slices (indicated from green to dark blue) are 1981-2000, 2021-2040, 2041-2060, 2061-2080, 2081-2100. The diagrams indicate the whole range of interannual variability (thinner lines), and the simulated values around the mean represented by the upper and lower quartiles (thicker boxes).

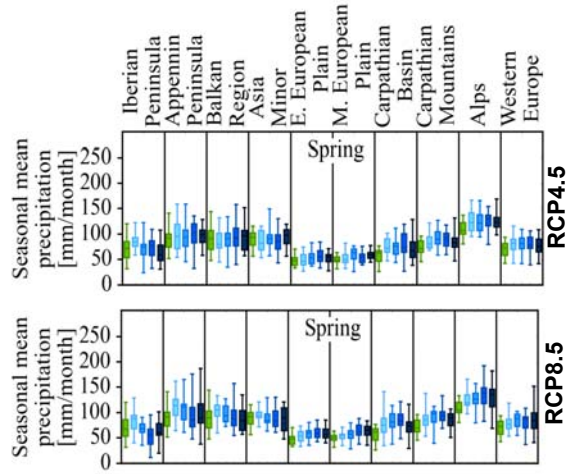

Fig. 8: Box-Whisker diagrams of spatial average values of spring (MAM) mean precipitation in the 10 subregions of the MED-44 CORDEX domain calculated from the RCP4.5 (top) and RCP8.5 (bottom) scenario experiments. The presented time slices (indicated from green to dark blue) are 1981-2000, 2021-2040, 2041-2060, 2061-2080, 2081-2100. The diagrams indicate the whole range of interannual variability (thinner lines), and the simulated values around the mean represented by the upper and lower quartiles (thicker boxes).

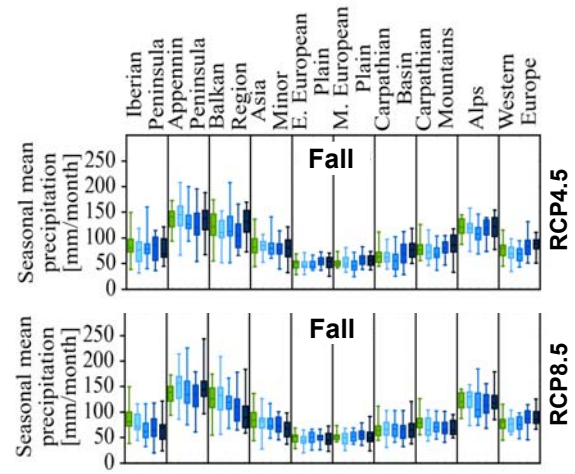

Fig. 10: Box-Whisker diagrams of spatial average values of fall (SON) mean precipitation in the 10 subregions of the MED-44 CORDEX domain calculated from the RCP4.5 (top) and RCP8.5 (bottom) scenario experiments. The presented time slices (indicated from green to dark blue) are 1981-2000, 2021-2040, 2041-2060, 2061-2080, 2081-2100. The diagrams indicate the whole range of interannual variability (thinner lines), and the simulated values around the mean represented by the upper and lower quartiles (thicker boxes).

Acknowledgements. Research leading to this paper has been supported by the following sources: the Hungarian Scientific Research Fund under grants K-78125, K-83909, and K109109, the AGRÁRKLIMA2 project (VKSZ_12-1-2013-0034), and the EEA Grant HU04 Adaptation to Climate Change Programme (EEA-C13-10).

REFERENCES

Bartholy, J., Pongrácz, R., Torma, Cs., Pieczka, I., Hunyady, A., 2009: Regional climate model experiments for the Carpathian basin. In: *Proceedings, 89th AMS Annual Meeting*. Phoenix, AZ. Paper 13A.03, 5p. Available online at http://ams.confex.com/ams/pdfpapers/147084.pdf

Bartholy, J., Pongrácz, R., Pieczka, I., Kelemen, F.D., Kis, A., André, K., 2015: Regional climate model experiment using RegCM subgridding options in the framework of Med-CORDEX. In: *Proceedings, 95th AMS Annual Meeting*. Phoenix, AZ. Paper 591, 6p. Available online at https://ams.confex.com/ams/95Annual/web-program/Manuscript/Paper262821/BJ-et-al-AMS 2015.pdf

Dickinson, R., Errico, R., Giorgi, F., Bates, G., 1989: A regional climate model for the western United States. *Clim. Chang.*, 15, 383-422.

Dickinson, R.E., Henderson-Sellers, A., Kennedy, P.J., 1993: Biosphere-atmosphere Transfer Scheme (BATS) Version 1e as Coupled to the NCAR Community Climate Model. *NCAR Technical Note* NCAR/TN-387+STR, DOI: 10.5065/D67 W6959

Elguindi, N., Bi, X., Giorgi, F., Nagarajan, B., Pal, J., Solmon, F., Rauscher, S., Zakey, A., Giuliani, G., 2011: Regional climatic model RegCM user manual version 4.3. 32p. ITCP, Trieste, Italy.

Giorgi, F., 1989: Two-dimensional simulations of possible mesoscale effects of nuclear war fires. 1. Model description. *J. Geophys. Res*., 94, 1127-1144.

Giorgi, F., Marinucci, M.R., Bates, G.T., 1993a: Development of a second generation regional climate model (RegCM2). Part I: Boundary layer and radiative transfer processes. *Mon. Wea. Rev.* 121, 2794-2813.

Giorgi, F., Marinucci, M.R., Bates, G.T., DeCanio, G., 1993b: Development of a second generation regional climate model (RegCM2). Part II: Convective processes and assimilation of lateral boundary conditions. *Mon. Wea. Rev.* 121, 2814-2832.

Giorgi, F., Mearns, L.O., 1999: Introduction to special section: regional climate modeling revisited *J. Geophys. Res.* 104, 6335-6352.

Giorgi, F., Francisco, R., Pal, J., 2003: Effects of a subgrid-scale topography and land use scheme on the simulation of surface climate and hydrology. Part I: Effects of temperature and water vapor disaggregation. *J. Hydrometeor.*, 4(2): 317-333.

Nakicenovic, N., Swart, R., Eds., 2000: *Emissions Scenarios.* A Special Reports of IPCC Working Group III, Cambridge University Press, Cambridge, UK. 570p.

Pal, J.S., Small, E., Elthair, E., 2000: Simulation of regionalscale water and energy budgets: representation of subgrid cloud and precipitation processes within RegCM. *J. Geophys. Res.* 105(29), 567-594.

Pongrácz, R., Bartholy, J., Kovács, G., Torma, Cs., 2010: Analysis of simulated mean and extreme climate trends for the Eastern/Central European region based on RegCM outputs using A1B scenario. *90th AMS Annual Meeting*. http://ams.confex.com/ams/pdfpapers/158358.pdf

Somot, S., Ruti, P., and the MedCORDEX modelling Team, 2012: The Med-CORDEX initiative: towards fully coupled Regional Climate System Models to study the Mediterranean climate variability, change and impact. *Geophysical Research Abstracts*, 14, EGU2012-6080

Torma, Cs., Coppola, E., Giorgi, F., Bartholy, J., Pongrácz, R., 2011: Validation of a high resolution version of the regional climate model RegCM3 over the Carpathian Basin. *J. Hydrometeor.*, 12, 84-100.

van Vuuren, D.P., Edmonds, J.A., Kainuma, M., Riahi, K., Thomson, A.M., Hibbard, K., Hurtt, G.C., Kram, T., Krey, V., Lamarque, J.-F., Masui, T., Meinshausen, M., Nakicenovic, N., Smith, S.J., Rose, S., 2011: The representative concentration pathways: an overview. *Climatic Change*, 109, 5-31. DOI: 10.1007/s10584-011-0148-z.